J Mater Sci: Mater Med (2011) 22:721–729
DOI 10.1007/s10856-010-4225-z

Preparation of magnetic and bioactive calcium zinc iron silicon oxide composite for hyperthermia treatment of bone cancer and repair of bone defects

Yumin Jiang · Jun Ou · Zhanhe Zhang · Qing-Hua Qin

Received: 6 September 2010 / Accepted: 21 December 2010 / Published online: 8 January 2011

Abstract In this paper, a calcium zinc iron silicon oxide composite (CZIS) was prepared using the sol–gel method. X-ray diffraction (XRD) was then employed to test the CZIS composite. The results from the test showed that the CZIS had three prominent crystalline phases: $Ca_2Fe_{1.7}Zn_{0.15}Si_{0.15}O_5$, Ca_2SiO_4, and $ZnFe_2O_4$. Calorimetric measurements were then performed using a magnetic induction furnace. Scanning electron microscopy (SEM) and energy dispersive spectroscopy (EDS) analysis were conducted to confirm the growth of a precipitated hydroxyapatite phase after immersion in simulated body fluid (SBF). Cell culture experiments were also carried out, showing that the CZIS composite more visibly promoted osteoblast proliferation than $ZnFe_2O_4$ glass ceramic and HA, and osteoblasts adhered and spread well on the surfaces of composite samples.

Y. Jiang · J. Ou (✉)
College of Materials Science & Engineering,
Guilin University of Technology, Guilin 541004,
People's Republic of China
e-mail: gloujun123@gmail.com

Y. Jiang
e-mail: jiangyumin2@yahoo.cn

Z. Zhang
The Second People's Hospital of Guilin, Guilin 541004,
People's Republic of China
e-mail: zzh941115@yahoo.com.cn

J. Ou
Key Laboratory of New Processing Technology for Nonferrous Materials, Ministry of Education, Guilin University of Technology, Guilin 541004, People's Republic of China

Q.-H. Qin
School of Engineering, Australian National University,
Canberra, ACT 0200, Australia
e-mail: qinghua.qin@anu.edu.au

1 Introduction

Cancer cells have a poorly developed nervous system and an insufficient matrix of blood vessels. The cells generally perish around 43°C due to hemorrhage, stasis and vascular occlusion [1]. normal cells, however, are not damaged below 45°C [2]. Therefore hyperthermia at between 43 and 45°C is expected to be one of the most useful treatments of bone cancer, without or with very little side effects [3]. According to the method of heating, the hyperthermia treatment can be classified as microwave thermotherapy, RF thermotherapy, ultrasonic thermotherapy, laser thermotherapy, extracorporeal whole body hyperthermia, circular heating medium thermotherapy, and magnetic thermoseed thermotherapy. To achieve the ideal effect of additives to thermotherapy, the following three conditions should be satisfied: (1) the tumor tissue is heated to above 43°C within a specified time and then kept at that temperature for another given time; (2) then, the temperature of the heated tumor tissues is kept at and above 41°C, which is the minimum temperature of hyperthermia treatment; (3) the temperature of the surrounding normal cells is kept below 45°C [4]. The main challenge of the hyperthermia treatment is how to measure and then precisely control the temperature in deep tissues. The use of thermally sensitive material such as zinc ferrite is expected to be helpful for identifying and controlling the temperature in hyperthermia treatments of cancer. For cancer tumors of deep tissues, such as osteocarcinoma, many magnetic glass–ceramic systems are used as thermoseed hyperthermia treatments of cancer, for example, $CaO–SiO_2–Fe_2O_3$

[5], MgO–CaO–SiO_2–P_2O_5–Fe_2O_3 [6], FeO–Fe_2O_3–CaO–SiO_2 [7], ZnO–Fe_2O_3–CaO–SiO_2 [3], SiO_2–Na_2O–CaO–P_2O_5–FeO–Fe_2O_3 [8], Li_2O–MnO_2–CaO–P_2O_5–SiO_2 [9], Fe_2O_3–CaO–ZnO–SiO_2–B_2O_3 [10], magnetite/hydroxyapatite composite [11] and CaO–SiO_2–P_2O_5–Na_2O–Fe_2O_3 [12]. To the authors' knowledge, however, reports on the study of magnetic calcium zinc iron silicon oxide composites (CZIS) are very limited in the literature. This is the motivation of this study. In this study, a magnetic composite of CZIS is synthesized using the sol–gel method. The structures of its final compound powders are then investigated by means of XRD. Calorimetric measurement of the samples, which is an important part of the experiment, is performed by way of a magnetic induction furnace. The bioactivity and in vitro cytocompatibility of the material are investigated using simulated body fluid (SBF) immersion, osteoblast morphologic observation, and cell viability assessment.

2 Materials and methods

2.1 Synthesis

The synthesis process included preparation of the zinc iron complex compound solution, the CZIS precursor gel, and the CZIS composite samples.

A schematic diagram of the synthesis process was shown in Fig. 1.

2.1.1 Preparation of zinc iron complex compound solution

The zinc iron complex compound solution was prepared by dissolving $Fe(NO_3)_3{\cdot}9H_2O$ and $Zn(NO_3)_2{\cdot}6H_2O$ in citric acid. The mole ratio of (Fe + Zn) to citric acid was 1:1. The mole ratios of Fe: Zn of the four samples were 1.7:0.21 (#1), 1.7:0.19 (#2), 1.7:0.17 (#3), 1.7:0.15 (#4), respectively.

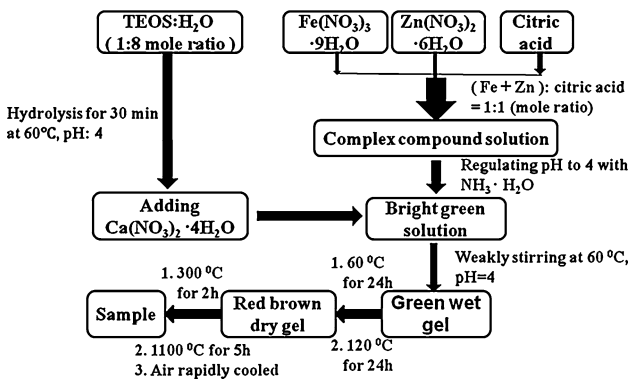

Fig. 1 Schematic diagram of preparation of CZIS composite

2.1.2 Preparation of CZIS precursor gel

At first, tetraethyl orthosilicate (TEOS) was slowly added to HNO_3 solution (pH = 4) at the mole ratio of 1:8 (TEOS: H_2O). The TEOS was hydrolysed for 30 min at 60°C with strong stirring. Then, aqueous solutions of $Ca(NO_3)_2{\cdot}4H_2O$ and zinc iron complex compound solution were added to the solution and stirred constantly until the gel was formed. Finally, the wet gel was aged at 60°C for 24 h. The respective quantities were showed in Table 1.

2.1.3 Preparation of CZIS composite samples

The wet gel (CZIS precursor gel) was dried at 120°C for 24 h. Then, the dry gel was ignited at 300°C to let the organic phases to be in a muffle furnace. Finally, the powders were calcined at 1100°C for 5 h at 5°C min^{-1} heating rate and then rapidly cooled in air. The CZIS composite samples were thus synthesized by the steps described above.

2.2 Characterization

In the characterization process, the structures of the samples prepared above were investigated by means of XRD (X'Pert PRO, Panalytical, Holland). In particular, the particle sizes of the samples were measured using a particle size and zeta potential analyzer (ZS90, Malvern, UK). Calorimetric measurement of the sample was performed using a magnetic induction furnace (LH30C, Lihua, China). Finally, the bioactivity of the material was investigated via SBF study and osteoblast adhesion study, and the cytotoxicity was evaluated by the MTT (succinate dehydrogenase activity, MTT) method. Each of these processes was described in detail as follows.

2.2.1 X-ray diffraction

The powders were subjected to powder XRD using Cu-Kα radiation. In the powder XRD, the X-ray power, scanning rate, and sampling angle were set at 40 kV–40 mA, 10°/min, and 0.01°, respectively. The crystalline phases in the powders were identified by referring to the data of the ICSD PDF2004.

2.2.2 Particle size analysis

The particle size of sample was measured using a particle size and zeta potential analyzer (ZS90, Malvern, UK). The measurement conditions were set as follows: Dispersant name: water, Material Rl: 2.00, Dispersant Rl: 1.330, Viscosity (cP): 0.8859.

Table 1 The respective quantities and purity of reagents

	Citric acid/g	$Zn(NO_3)_2{\cdot}6H_2O$/g	$Fe(NO_3)_3{\cdot}9H_2O$/g	H_2O/ml	TEOS/ml	$Ca(NO_3)_2{\cdot}4H_2O$/g
#1	28.6634	4.6121	50.7022	1.54	8.49	35.3281
#2	28.6632	4.1727	50.7021	1.54	8.49	35.3282
#3	28.6633	3.7335	50.7023	1.54	8.49	35.3280
#4	28.6631	3.2943	50.7020	1.54	8.49	35.3281
Purity	AR	AR	AR	pH = 4	AR	AR

2.2.3 *Calorimetric measurements*

Calorimetric measurements were carried out in the manner described in [1]. A magnetic induction furnace was used at a magnetic field 500 Oe and frequency 400 kHz. Two grams of CZIS composite powder and $ZnFe_2O_4$ glass ceramics (30 wt% iron, self-made by the melt-quench method using oxy-acetylene flame) were separately placed at the center of the coil in 20 ml deionized water in a quartz cuvette under a magnetic field 500 Oe and frequency 400 kHz for 3 min. Initial and final temperatures were measured using a thermometer (0–100°C, the minimum scale is 0.1°C). The specific power loss is calculated using the formulation:

$$P = m_w c_w \Delta T/(tm) \quad (1)$$

where P was the specific power loss (W/g), t the time (180 s in our work); m the sample's mass (2 g), m_w the water mass (20 g); c_w the water specific heat capacity (4.2 J/g°C) and ΔT the temperature variation.

2.2.4 *Bioactivity*

2.2.4.1 Soaking in SBF As shown in Table 2, 1000 ml SBF (1.5 mg/ml) was prepared. Then the pH of the SBF was regulated to 7.4 using tris(hydroxymethyl)aminomethane (THAM) and hydrochloric acid.

The CZIS composite flake samples, which were formed with a cold pressing process at 10 MPa, were immersed in SBF at the rate of 1:10 surface area (mm^2)/volume (ml). The soaking conditions were as follows: 37°C water-bathing for 1, 2 and 4 weeks, replacing the SBF every 4 days. Samples which had been soaked in SBF for a given time were cleaned with deionized water and pure ethanol, and dried at room temperature. Undefiled samples were subsequently sputter-coated with carbon for scanning electron microscopy (SEM, JSM-6380LV, JEOL, Japan) and energy dispersive X-ray spectroscopy (EDS, 7582, Oxford, U.K.) analysis. SEM and EDS were used to validate the growth of the precipitated hydroxyapatite phase after soaking in SBF.

Table 2 Reagent and sequence of SBF preparation

Sequence	Reagent	Addition amount (g)
1	NaCl	8.0028
2	$NaHCO_3$	0.3528
3	KCl	0.2238
4	$K_2HPO_4{\cdot}3H_2O$	0.2282
5	$MgCl_2{\cdot}6H_2O$	0.3045
6	$CaCl_2$	0.2775
7	Na_2SO_4	0.0710

2.2.4.2 Osteoblast adhesion Osteoblast culture. Osteoblasts were isolated by sequential trypsin-collagenase-hyaluronidase digestion on the shank of 3-month-old Sprague–Dawley rats supplied by Guilin Medical University. Briefly, the shank was dissected and freed from soft tissue, cut into small pieces under aseptic conditions, and rinsed in calcium and magnesium free phosphate-buffered saline (PBS). To minimize fibroblastic contamination and cell debris, the shank pieces were incubated in a 0.25% trypsin enzyme solution for 20 min, followed by five sequential digestive processes with 0.2% collagenase and 0.1% hyaluronidase in a metabolic shaker at 37°C for 60 min each. The first and second supernatants were collected. After continuous enzyme treatment, the supernatants were centrifuged at 300 g for 10 min, and the pellets were resuspended in Ham's F-12 culture medium supplemented with 10% fetal bovine serum (FBS) and maintained in a controlled humidified chamber at 37°C with 5% CO_2. Media were changed every other day until the cells reach confluence. The cells used in this study were between the second and fourth passages.

Osteoblast morphologic observation. For evaluation of cell adhesion on the CZIS, tablets were prepared at 10 MPa with a tablet machine. Sterilized tablets were placed in the bottom of each well of a 24-well tissue-culture plate. Osteoblasts were seeded on each pellet at a density of 1×10^4 cells/cm^2 and incubated for 1 and 3 days in Ham's F-12 culture medium in a controlled humidified chamber at 37°C and 5% CO_2. After prescribed culture times, samples

were removed from the culture wells, fixed in 2.5% glutaraldehyde in 0.1 M sodium cacodylate buffer (pH = 7.4) for 1 h, rinsed with PBS three times and dehydrated in ethanol. Samples were sputter coated for SEM analyses.

2.2.5 Cell viability assay

It was widely accepted that in vitro testing procedures were of considerable importance in cytotoxicity investigations of biomaterials. Based on the International Standard (ISO 10993-5) method, MTT could be applied in this evaluation. In brief, the CZIS composite samples, $ZnFe_2O_4$ glass ceramic and HA were separately ground and sieved through a 60-mesh sieve; granules with a size range (100–600 μm) were then used as testing materials. All specimens were sterilized overnight with dry heat at 180°C. Under sterile conditions, samples were immersed in the culture medium in a humidified atmosphere of 5% CO_2 and 95% air. The ratio of powder weight (mg) to the medium (F-12) volume (ml) was 200 mg/ml. After incubating at 37°C for periods of 2, 4, 8, 16, 24, 48 and 72 h, the suspension was centrifuged, and the supernatant collected as extracts. To investigate the changes of ions in the medium, the Si, Fe, Zn, and Ca ionic concentrations of the extraction liquids were measured using ICP-AES. Extracts from them (24, 48, 72 h) were used for MTT assays. Osteoblasts were harvested and the cell suspension is adjusted to a density of 1.0×10^4 cells/cm^2; then 100 μl of the cell suspension was added to each well of a 96-well plate. After incubation at 37°C for 24 h, the culture medium was removed and replaced by 50 μl of extract and 50 μl F-12 of medium supplemented with 10% FBS. The cells were cultured in vitro with the extracts, and after incubation in 95% air humidity and 5% CO_2 at 37°C for 1, 2, 3 and 5 days, respectively, the 3-(4, 5-dimethylthiazol-2-yl)-2, 5-diphenyl tetrazolium bromide solution was added to each well (100 μl per well of a 0.5 mg/ml MTT solution in PBS) and the mixture incubated for 4 h at 37°C. The supernatant was removed and insoluble formazan crystals were dissolved in 100 μl dimethylsulfoxide (DMSO) in each well. The optical density was measured at 570 nm using a microplate reader (EL × 800, BIO-TEK). For the MTT experiment, three sample groups (HA: HA-24, HA-48, HA-72; $ZnFe_2O_4$ glass ceramic: ZFG-24, ZFG-48, ZFG-72; CZIS samples: CZIS-24, CZIS-48, CZIS-72) were tested, with a complete liquid culture medium as negative or nontoxic control, for different durations (1, 2, 3, 5 days). Two independent experiments were performed with four samples per group ($n = 4$). The mean values ± standard deviation of absorbance values obtained from cells incubated in the presence of the extracts, either from controls or material extracts, were calculated. Results for the MTT assays were expressed as the percentage of the corresponding negative control conducted in the same experiment. Statistical analysis was performed by one-way analysis of variance (ANOVA) with Tukey–Kramer post-tests for comparison of multiple means. A P-value < 0.05 was considered statistically significant.

3 Results and discussion

3.1 Powder X-ray diffraction

From the XRD image of the CZIS composite sample (Fig. 2) it was found that the material contains three prominent crystalline phases: calcium zinc iron silicon oxide ($Ca_2Fe_{1.7}Zn_{0.15}Si_{0.15}O_5$) (ICSD PDF2004: 00-045-0569), dicalcium silicate (Ca_2SiO_4) (ICSD PDF2004: 01-086-0401), and zinc ferrite ($ZnFe_2O_4$) (ICSD PDF2004: 01-079-1150). The peak intensity of the $ZnFe_2O_4$ increased along with an increase in the Zn content. Conversely, the peak intensity of the $Ca_2Fe_{1.7}Zn_{0.15}Si_{0.15}O_5$ decreased with an increase in the Zn content, and the reason was the increase in Zn–Fe interactions. The strongest peak of the $Ca_2Fe_{1.7}Zn_{0.15}Si_{0.15}O_5$ was evident in #4, and its content was about 64% by semi-quantitative calculation (Table 3). The $ZnFe_2O_4$ exhibited ferrimagnetism due to the random distribution of Fe^{3+} and Zn^{2+} ions at tetrahedral A sites and octahedral B sites. This inversion/random distribution

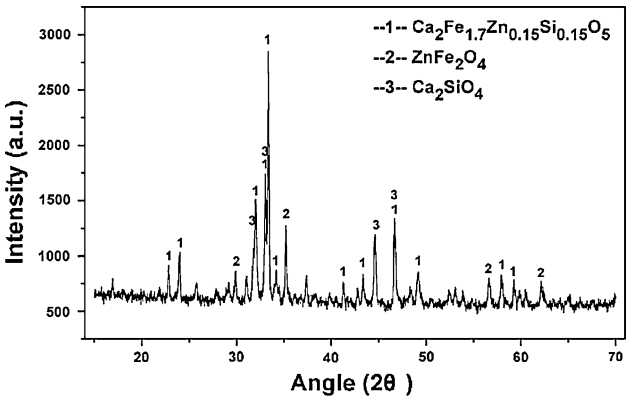

Fig. 2 XRD image of CZIS composite sample

Table 3 The prominent crystalline phase contents of the four samples

	$Ca_2Fe_{1.7}Zn_{0.15}Si_{0.15}O_5$/%	$ZnFe_2O_4$/%	Ca_2SiO_4/%	Impurity/%
#1	48.5	6	39.4	6.1
#2	52	8	35	5
#3	58	9.1	26	6.9
#4	64.3	10.8	19.8	5.1

of ions were probably attributable to the surface effects of nano-$ZnFe_2O_4$ and rapid cooling of the material from 1100°C (thus preserving the high temperature state of the random distribution of ions) [1, 3]. The $ZnFe_2O_4$ in our material met all demands of the experiment (rapid cooling of the material from 1100°C and surface effects of nano-$ZnFe_2O_4$). Thus, we deduced that the $ZnFe_2O_4$ in our material was ferromagnetic, whereas the Ca_2SiO_4 phase was bioactive and osteoinductive [13, 14]. As a result, both the Ca_2SiO_4 and $ZnFe_2O_4$ phases had no adverse impact on the magnetism and bioactivity of the whole sample.

3.2 Particle size analysis

Figure 3 showed the particle size distribution of the CZIS composite sample. The particle size distribution was in the range of 458.7–955.4 nm, and the average diameter was 871.6 nm. The reason for the wide particle size distribution was hydration of the dicalcium silicate (Ca_2Si0_4) to some degree. The size of the submicron particles ranged from 128 to 525 nm, and these particles could be located near a tumor to provide treatment for cancer [15]. Thus, particles broken off from CZIS matrix can be delivered into tumor cells via endocytosis.

3.3 Calorimetric measurements

It was evident from Fig. 4 that the maximum specific power loss and temperature of the CZIS samples #4 increased, respectively, to 7 W/g and 30°C after 3 min at 20°C room temperature. But the power loss and temperature were still lower than those of $ZnFe_2O_4$ glass ceramic. It was also found from Fig. 4 and Table 3 that the $ZnFe_2O_4$ was ferrimagnetic in the CZIS samples. The $ZnFe_2O_4$ was therefore beneficial to the specific power loss and temperature increase of CZIS samples. $ZnFe_2O_4$ exhibited ferrimagnetism due to the random distribution of Zn^{2+} and Fe^{3+} cations at tetrahedral A sites and octahedral B sites [1]. The rapid cooling of the material from 1100°C in an air–water furnace resulted in this inversion/random distribution of cations. Considering these experimental results, it can be estimated that 2 g of our material implanted in a

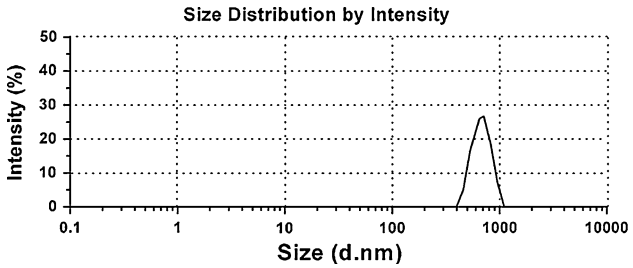

Fig. 3 Particle size distribution of CZIS composite sample

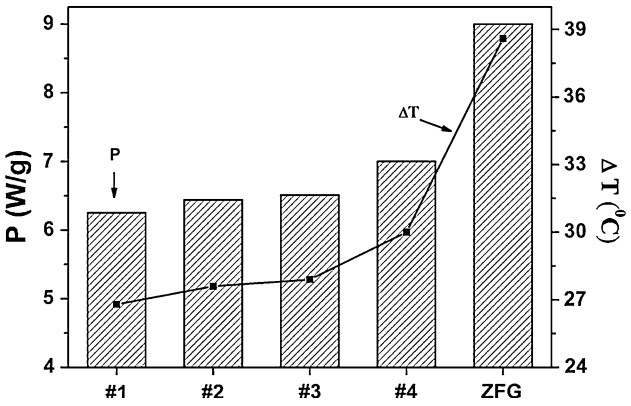

Fig. 4 Variations of specific power loss (P) and temperature increase (ΔT)

tumor might produce a maximum temperature of 50°C around the tumor. The temperature variation was influenced by the sample's mass, magnetic field strength, and tissue characteristics (blood flow, tissue depth, tissue density, and type of cancer).

3.4 Bioactivity

3.4.1 Soaking in SBF

Figure 5 showed the growth of precipitated layers on the surfaces of CZIS samples after immersion in SBF for 1 week (Fig. 5a), 2 weeks (Fig. 5b) and 4 weeks (Fig. 5c). A precipitated layer appeared after 1 week's immersion. The depth of the layer increased with an increase in soaking time, and was most prominent after 4 weeks' immersion. Figure 6 confirmed that the peaks of the precipitated layers' Ca and P gradually increased, whereas the peaks of Si and Zn gradually decreased after 4 weeks' immersion. This phenomenon was attributed to the degradation of Ca_2SiO_4 and $ZnFe_2O_4$. According to the EDS data of the precipitated layers in Table 4, the ratio of Ca/P decreased as soaking duration increases. When soaking time reaches 4 weeks, the ratio of Ca/P was 1.68, and it gradually approached 1.67 (apatite formation). From these results it could be concluded that the precipitated layer on the CZIS sample's surface in this study was carbonated hydroxyapatite or bone-like apatite (Figs. 5, 6 , Table 4).

3.4.2 Observation of cell morphology

A typical osteoblast attachment to the surface of the CZIS sample after 1 day in culture was shown in Fig. 7a. The cells exhibited a higher density, with dorsal ruffles and minor filopodia apparent on the surface of the CZIS sample tablet after 3 days in culture (Fig. 7b). It was also evident that cells proliferate to form a monolayer. One possible explanation for cell attachment to the sample was that the

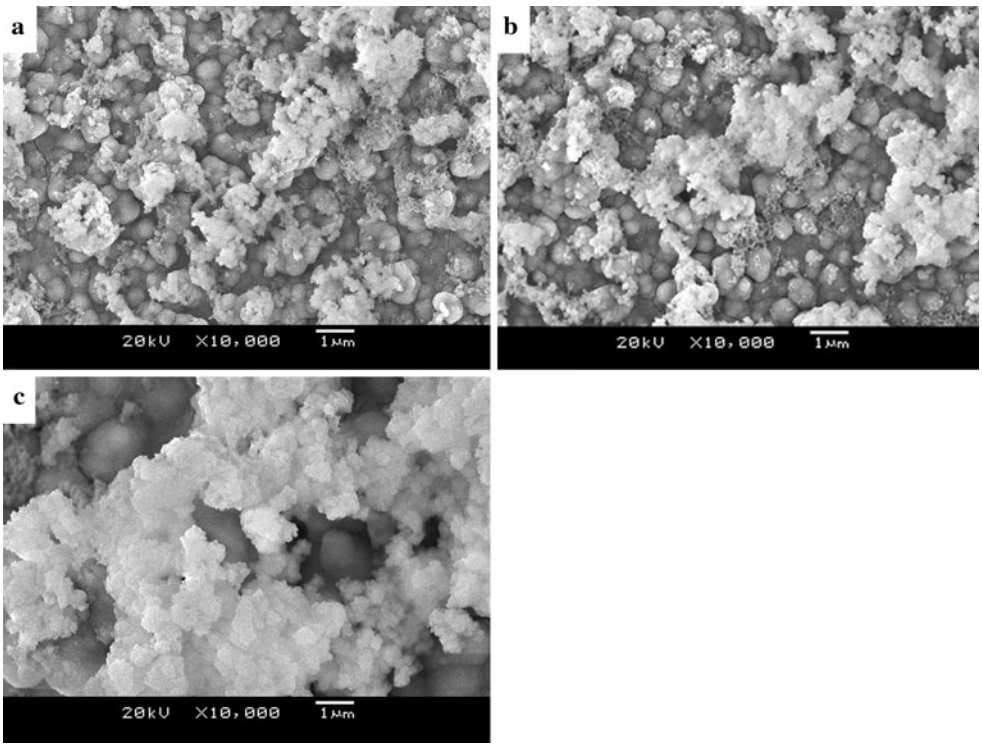

Fig. 5 SEM micrographs of CZIS composite samples after **a** 1 week, **b** 2 weeks, **c** 4 weeks of immersion in SBF

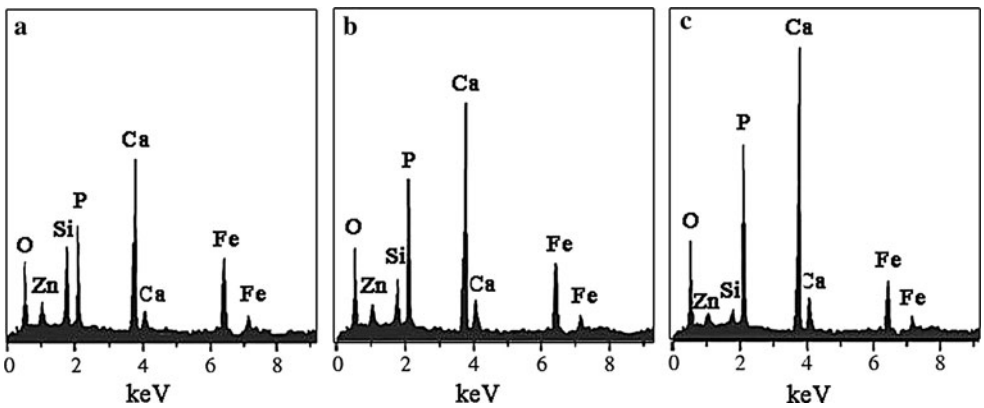

Fig. 6 EDS images of CZIS composite samples after **a** 1 week, **b** 2 weeks, **c** 4 weeks of immersion in SBF

released ions promote cell adhesion by mediating cellular integrin interactions associated with signal transduction pathways [16]. Further studies were needed to confirm this hypothesis. The present experimental results demonstrated that the CZIS sample was beneficial for the attachment and proliferation of osteoblast cells.

3.5 Cell viability assay

Osteoblast viability and proliferation were measured by the MTT assay. Cell proliferation with the CZIS sample extract was significantly different from that with the HA extract and $ZnFe_2O_4$ glass ceramic extract. A stronger trend of cellular viability and proliferation was observed for osteoblasts exposed to specific sample extract solutions (Fig. 8). Bioactive materials were shown to control cellular response via genetic alterations. For example, the specific ranges of silica released were found to promote the expression of growth factors that stimulate osteoblast differentiation [17, 18]. Cell proliferation with the CZIS sample extract was significantly superior to that with the HA extract and $ZnFe_2O_4$ glass ceramic extract. The reason may be related to the release of silicate ions, zinc ions and iron ions from the material. Extracts of other

Table 4 Elemental composition based on EDS analysis

	Element	Element weight (%)	Atom (%)	Ca/P
1 week	O	5.08	12.09	1.87
	Zn + Fe	35.51	23.16	
	Si	10.75	14.57	
	P	14.25	17.51	
	Ca	34.41	32.67	
2 weeks	O	5.48	12.83	1.72
	Zn + Fe	29.94	19.27	
	Si	6.38	8.52	
	P	18.05	21.84	
	Ca	40.15	37.54	
3 weeks	O	5.74	13.19	1.68
	Zn + Fe	23.34	14.76	
	Si	3.14	4.11	
	P	21.35	25.35	
	Ca	46.43	42.59	

[a] Other elements (e.g. H and C) which can't detect by our EDS, are ignored

silicon-substituted biomaterials had been shown to modulate cellular activity [16]. But the actions of zinc ions and iron ions in promoting cellular activity have not been clarified. Therefore, further study of this method is required.

4 Conclusion

In this paper magnetic and bioactive CZIS samples are prepared using a sol–gel method. The CZIS composite was then tested using XRD. It is found that the CZIS composite has three prominent crystalline phases: $Ca_2Fe_{1.7}Zn_{0.15}Si_{0.15}O_5$, Ca_2SiO_4, and $ZnFe_2O_4$ (ferrimagnetism). Measurements of the particle size of the CZIS were also conducted. The results showed that the particle size distribution the CZIS sample was in the range of 458.7–955.4 nm and their average diameter was 871.6 nm. Further, calorimetric measurements were carried out using a magnetic induction furnace at 500 Oe magnetic field and 400 kHz frequency. The results showed that the specific power loss and temperature increase of the CZIS samples were, respectively, 7 W/g and 30°C after being maintained for 3 min at 20°C room temperature, which can met the requirements of hyperthermia treatment. The specific power loss and temperature increase of the CZIS are lower than those of the $ZnFe_2O_4$ glass ceramic. SEM and EDS analyses were conducted, the results confirming the growth of a precipitated hydroxyapatite phase after immersion in SBF; the cell culture experiment results showed that the CZIS composite more visibly promoted osteoblast proliferation than $ZnFe_2O_4$ glass ceramic and HA, and the osteoblasts adhered and spread well on the surface of the CZIS composite, suggesting that the magnetic CZIS composite was bioactive.

Although the specific power loss and temperature increase of the CZIS were both lower than those of $ZnFe_2O_4$ glass ceramic, the specific power loss and temperature increase of the CZIS met the needs of hyperthermia treatment, and the biological activity and osteoblast induction of the CZIS exceeded both $ZnFe_2O_4$ glass ceramic and HA. Thus, the CZIS composite was magnetic and bioactive, and achieved the expected target. It will be a promising material for hyperthermia treatment of bone cancer and repair of bone defects.

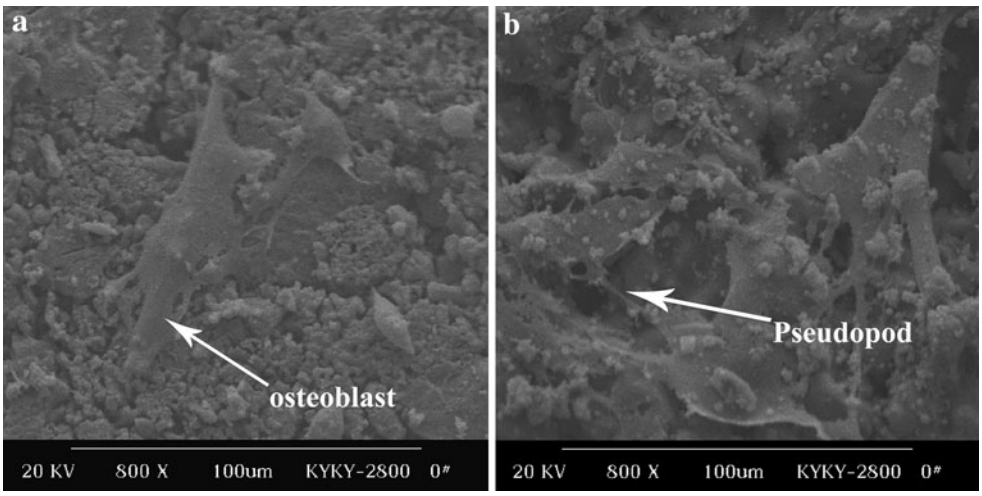

Fig. 7 Morphology of osteoblasts cultured on CZIS composite sample tablet **a** 1 day, **b** 3 days

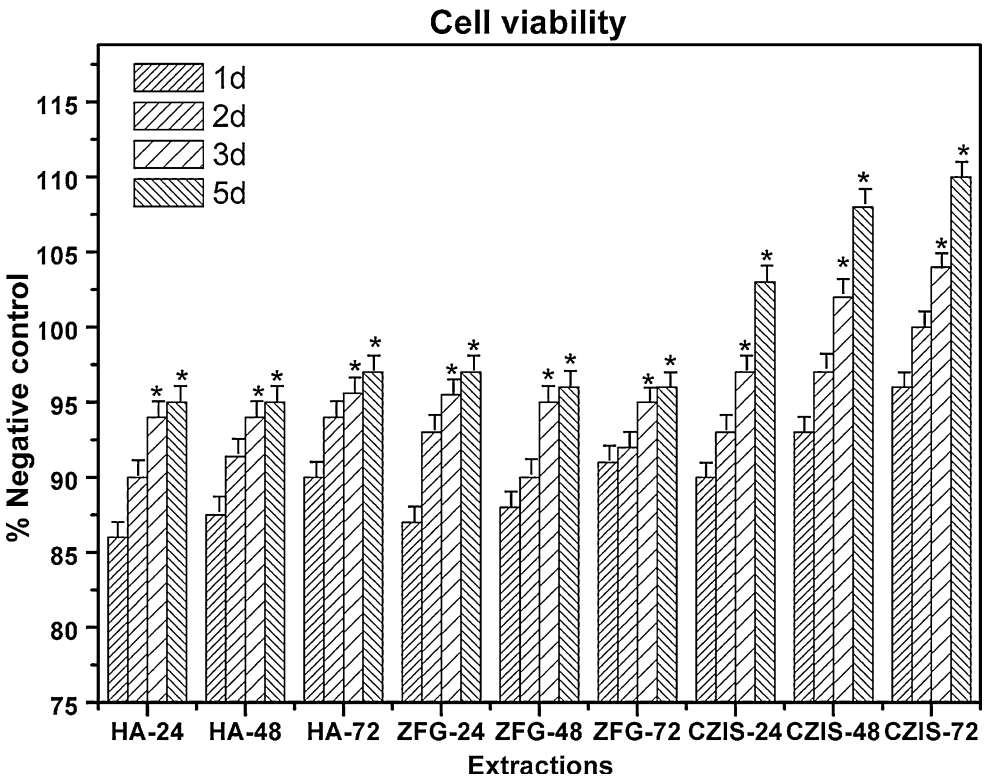

Fig. 8 Osteoblast proliferation, as measured by the MTT assay, following 1, 2, 3 and 5 days in culture with CZIS composite sample extract, $ZnFe_2O_4$ glass ceramics and HA extract, collected after 24, 48 and 72 h. Data are expressed as percentages of the control value for initial cell seeding (*$P < 0.05$)

Acknowledgments The authors gratefully acknowledge the assistance of Mr. George at Guilin University of Technology in preparing the manuscript. Support from the Guangxi Natural Science Foundation (No. 2008GXNSFC 0832021 and No. 2010GXNSFA013031) and the Key Project of Medical and Health of Guangxi (No. 2010056) is also fully acknowledged.

References

1. Shah SA, Hashmi MU, Alam S, Shamim A. Magnetic and bioactivity evaluation of ferrimagnetic $ZnFe_2O_4$ containing glass ceramics for the hyperthermia treatment of cancer. J Magn Magn Mater. 2010;322:375–81.
2. Roemer RB. Engineering aspects of hyperthermia therapy. Annu Rev Biomed Eng. 1999;1:347–76.
3. Kawashita M, Iwahashi Y, Kokubo T, Yao T, Hamada S, Shinjo T. Preparation of glass-ceramics containing ferrimagnetic zinc-iron ferrite for the hyperthermal treatment of cancer. J Ceram Soc Jpn. 2004;112:373–9.
4. Li J. Physics of tumor hyperthermia. Beijing: Science Publisher; 2008. p. 1–6.
5. Ebisawa Y, Kokubo T, Ohura K, Yamamuro T. Bioactivity of Fe_2O_3-containing CaO–SiO_2 glasses: in vitro evaluation. J Mater Sci: Mater Med. 1993;4:225–32.
6. Singh RK, Srinivasan A. Bioactivity of ferrimagnetic MgO–CaO–SiO_2–P_2O_5–Fe_2O_3 glass-ceramics. Ceram Int. 2010;36:283–90.
7. Ebisawa Y, Miyaji F, Kokubo T, Ohura K, Nakamura T. Bioactivity of ferrimagnetic glass-ceramics in the system FeO–Fe_2O_3–CaO–SiO_2. Biomaterials. 1997;18:1277–84.
8. Bretcanu O, Verné E, Cöisson M, Tiberto P, Allia P. Magnetic properties of the ferrimagnetic glass-ceramics for hyperthermia. J Magn Magn Mater. 2006;305:529–33.
9. His CS, Cheng HZ, Hsu HJ, Chen YS, Wang MC. Crystallization kinetics and magnetic properties of iron oxide contained $25Li_2O$–$8MnO_2$–20CaO–$2P_2O_5$–$45SiO_2$ glasses. J Eur Ceram Soc. 2007;27:3171–6.
10. Abdel-Hameed SAM, Hessien MM, Azooz MA. Preparation and characterization of some ferromagnetic glass-ceramics contains high quantity of magnetite. Ceram Int. 2009;35:1539–44.
11. Murakami S, Hosono T, Jeyadevan B, Kamitakahara M, Ioku K. Hydrothermal synthesis of magnetite/hydroxyapatite composite material for hyperthermia therapy for bone cancer. J Ceram Soc Jpn. 2008;116:950–4.
12. Singh RK, Kothiyal GP, Srinivasan A. Magnetic and structural properties of CaO–SiO_2–P_2O_5–Na_2O–Fe_2O_3 glass ceramics. J Magn Magn Mater. 2008;320:1352–6.
13. Chen CC, Ho CC, Chen CH, Wang WC, Ding SJ. In vitro bioactivity and biocompatibility of dicalcium silicate cements for endodontic use. J Endodont. 2009;35:1554–7.
14. Gandolfi MG, Ciapetti G, Perut F, Taddei P, Modena E, Rossi PL, Prati C. Biomimetic calcium-silicate cements aged in simulated body solutions. Osteoblast response and analyses of apatite coating. J Appl Biomater Biomech. 2009;7:160–70.
15. Santos-Roman N. Examination of the effect of PEG-rich matrices in Multi Drug Resistance-Associated Protein (MRP) and Multi Drug Resistance (MDR) substrates transport utilizing the CaCo-2 cell model. University of Puerto Rico; 2008.
16. Zreiqat H, Howlett CR, Zannettino A, Evans P, Schulze-Tanzil G, Knabe C, Shakibaei M. Mechanisms of magnesium-stimulated adhesion of osteoblastic cells to commonly used orthopaedic implants. J Biomed Mater Res. 2002;62:175–84.

17. Xynos ID, Edgar AJ, Buttery LDK, Hench LL, Polak JM. Ionic products of bioactive glass dissolution increase proliferation of human osteoblasts and induce insulin-like growth factor II mRNA expression and protein synthesis. Biochem Biophys Res Commun. 2000;276:461–5.

18. Silver IA, Deas J, Erecinska M. Interactions of bioactive glasses with osteoblasts in vitro: effects of 45S5 Bioglass®, and 58S and 77S bioactive glasses on metabolism, intracellular ion concentrations and cell viability. Biomaterials. 2001;22:175–85.